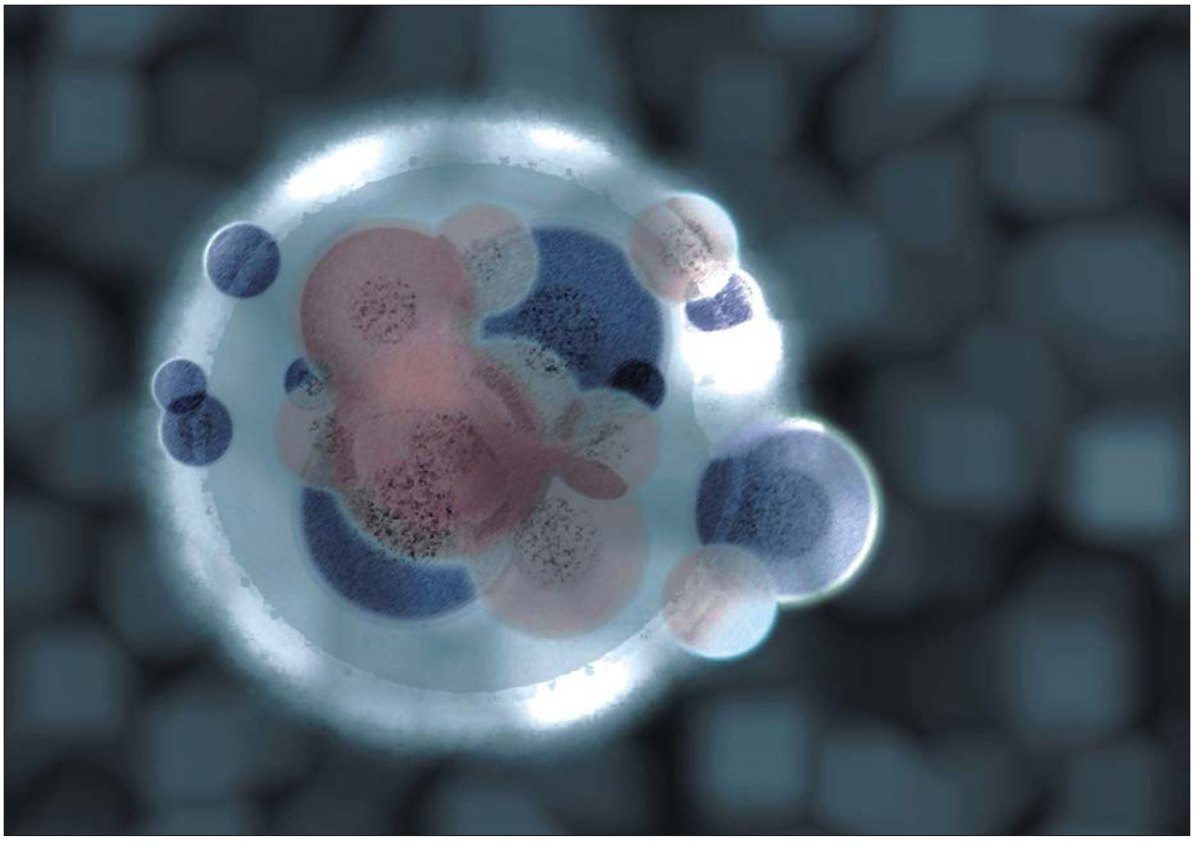

Journal of Biological Sciences

ISSN 1727-3048

science alert

ANSInet
an open access publisher
http://ansinet.com

Journal of Biological Sciences 12 (4): 232-238, 2012
ISSN 1727-3048 / DOI: 10.3923/jbs.2012.232.238

Spatial Variability of Orange Spotting Disease in Oil Palm

[1]S. Selvaraja, [1]S.K. Balasundram, [2]G. Vadamalai and [3]M.H.A. Husni
[1]Department of Agriculture Technology, [2]Department of Plant Protection,
[3]Department of Land Management, Faculty of Agriculture,
Universiti Putra Malaysia, 43400 Serdang, Selangor, Malaysia

Abstract: Orange Spotting (OS) disease which is caused by Cadang-Cadang Coconut Viroid (CCCVd) is an emerging problem in oil palm. This study was aimed at quantifying the spatial variability of OS disease severity as an effort to augment the effectiveness of OS phytopathometry appraisal. A 4.2 ha study plot was established in a commercial oil palm plantation at Sungai Buloh, Selangor. A total of 587 geo-referenced trees were visually observed for OS disease symptoms. OS disease severity data were first subjected to exploratory analysis and followed by variography and interpolation analyses to assess spatial variability. The incidence OS disease in the study area was 74.3%. Measured OS disease severity ranged from 0-92.3%. The spatial structure of OS disease severity was described by an exponential model with an effective range of 29.1 m. OS disease severity exhibited a strong spatial dependence with a nugget to sill ratio of 0.15. The spatial variability map of OS disease severity revealed spatial clustering of kriged values, where 73% of the study area showed low severity (1-30%), 25% showed moderate severity (30-60%) and approximately 2% showed high severity (> 60%). This study demonstrates the utility of geo-spatial information in understanding the OS disease severity scale which could assist in site-specific disease monitoring and intervention.

Key words: Oil palm, orange spotting disease, cadang-cadang coconut viroid, phytopathometry, spatial variability, precision agriculture

INTRODUCTION

Orange Spotting (OS) disease is becoming a significant problem in oil palm production. The causal agent of OS is Coconut Cadang-Cadang Viroid (CCCVd) which was first extracted from OS symptomatic palms in the Solomon Islands (Hanold and Randles, 1991).

Generally, CCCVd-infected oil palms exhibit orange spots on the fronds. The youngest fronds are typically free of spots. In young fronds, the irregular shape and non-necrotic orange spots are about 2-3 mm in diameter and occur between veins of the leaflets (Forde and Leyritz, 1968). The size and number of spots on fronds increase with palm age and in severe cases, distal necrosis can be observed on leaflets (Hanold and Randles, 1991).

In comparison to non-infected oil palms, OS-infected palms are relatively shorter and bear smaller fruit bunches, rendering infected palms as significantly less productive (Hanold and Randles, 1991). OS-infected palms yield 25-50% lower than the nearest healthy palms (Randles, 1998).

The natural mode of CCCVd transmission in oil palm is still unclear and several aspects of OS epidemiology are still unknown and need investigation (Randles and Rodriguez, 2003). OS disease incidence is related to oil palm age. Studies have shown that OS incidence is negligible in 10 year old palms but a significant linear regression of incidence on age has been observed for palms above 10 years of age (Sill *et al*., 1964; Price and Bigornia, 1971, 1972). OS incidence on mature palms ranges from 50-60%. Recently, OS incidence was observed in several Malaysian oil palm plantations. Vadamalai and Perera (2009) had identified several variants of CCCVd in a mature oil palm stand using ribonuclease protection assay and associated these variants to OS symptoms. While the cause of OS symptom is clear, there are currently no published reports on the severity of OS symptom particularly with regard to spatial distribution.

Accurate and precise quantitative disease measurement is a key step towards an integrated disease management program (Nutter *et al*., 2005). Quantification of spatial variability is a fundamental step in designing Precision Agriculture (PA) strategies for optimized crop and/or soil management (Balasundram *et al*., 2006a, b). Conceptually, PA is driven by a systems approach that promotes optimal input use at high-efficiency leading to sustainable production practices (Shibusawa, 1998). PA

Corresponding Author: S.K. Balasundram, Department of Agriculture Technology, Faculty of Agriculture, Universiti Putra Malaysia, 43400 Serdang, Selangor, Malaysia

strategies typically involve site- and time-specific treatments with regard to pest and disease control instead of the traditional prophylactic treatment. This approach is deemed to potentially reduce the cost of pest and disease control and its associated risks (Gebbers and Adamchuk, 2010).

Quantifying the spatial variability of pest and disease facilitates effective phytopathometry appraisals. The spatial dynamics of plant disease can be quantified by visually assessing disease severity (Nutter *et al*., 2005). Rekah *et al*. (1999) used spatial variability quantification on tomato crown and root rot disease to demonstrate the polycyclic nature of its causal agent, *Fusarium oxysporum* f. sp. *radicis-lycopersici* which is a deviation from the monocyclic nature of many non-zoosporic soilborne pathogens. Paulitz *et al*. (2003) performed a spatio-temporal variability assessment on the incidence of crown root rot on selected cereal crops to demonstrate an over-dispersed distribution of the pathogen, *Rhizoctonia oryzae*. Villate *et al*. (2008) quantified the spatial distribution of *Xiphinema index* which is the virus vector of grapevine fanleaf disease, to demonstrate a preferential direction of disease dispersal. Alves *et al*. (2009) used spatial variability assessment to visualize the severity of rust (*Hemileia vastatrix*) and brown eyespot (*Cercospora coffeicola*) in a coffee plantation. These diseases was found to be dispersed in a foci pattern within the coffee plantations. Cordier *et al*. (2011) quantified the spatial variability of phyllosphere fungal assemblages in beech (*Fagus sylvatica*) and found the spatial structure of phyllosphere fungal assemblage to be associated with genetic variation of beech trees.

This study is part of an on-going effort to develop a comprehensive phytopathometry appraisal protocol for OS disease in oil palm. Specifically, this study aimed at quantifying the spatial variability of OS disease severity in a mature oil palm stand.

MATERIALS AND METHODS

Study site: OS disease severity assessment was conducted in a commercial oil palm plantation located at Kuala Selangor, Peninsular Malaysia. The plantation is situated N 3.30°E 101.32° with a mean temperature of 27.3°C and a dew point of 23°C. OS disease severity was assessed in a 4.2 ha plot within a 40 ha management block which is designated as a performance research plot. The assessment plot is managed optimally in order to minimize yield-limiting factors.

Disease severity assessment: OS disease symptoms were visually observed on 587 mature oil palm trees in duration of 4 months that were planted in 1996. For each geo-referenced tree, the number of fronds with bright orange lesions and the total number of fronds were recorded. The percentage of disease severity for each tree was calculated as follows:

$$\text{Disease severity}(\%) = \frac{\text{No. of fronds with orange spotting symptoms}}{\text{Total No. of fronds per palm}} \times 100$$

Exploratory data analysis: OS disease severity data were subjected to Grubb's outlier test and descriptive statistics. Erratic disease severity values were omitted from further data analysis. Minimum, maximum, mean, standard deviation, variance, standard error and coefficient of variation for disease severity were computed using statistic version 8.1. The data were then assessed for normality using the Shapiro-Wilk test.

Spatial variability: There are two fundamental processes in geo-spatial statistics which are to: (1) model the uncertainty or error of the estimated surface (variography) and (2) describe spatial patterns by interpolating (kriging) sampled values. A variogram models the spatial continuity of a variable to enable characterization of spatial variability structure which is described by parameters such as nugget, sill and range. Kriging is a robust interpolation technique commonly used to generate maps (raster layers) from geo-referenced data (vector layers). Kriging utilizes the measured values and variogram model to compute estimated values from unsampled locations. Geo-statistical analysis requires the data to be continuous and trend-free. Prior to spatial analysis, the data is subjected to exploratory analysis. Typically, outliers are discarded and the outlier-free data are subjected to appropriate transformation if required.

The best variogram model is selected based on cross validation. Cross validation is performed using Mean Error (ME), Root Mean Square (RMSE) and Standardized Mean Squared Error (SMSE) (Delhomme, 1978; Merino *et al*., 2001). Cross validation statistics are computed as follows:

$$\text{ME} = \frac{1}{l}\sum_{j}^{l} = 1[\check{z}(S_j) - z(S_j)] \quad (1)$$

$$\text{RMSE} = \sqrt{\frac{1}{l}\sum_{j=1}^{l}[\check{z}(S_j) - z(S_j)]^2} \quad (2)$$

$$\text{SMSE} = \frac{1}{l} - 1\sum_{j=1}^{l}\frac{[\check{z}(S_j) - z(S_j)]^2}{\sigma^2} \quad (3)$$

Where:

l = No. of sampled points
$\check{z}(s_j)$ = Predicted value of the variable at point s_j
$z(s_j)$ = Measured value of the variable at point s_j
σ^2 = Theoretical variance

The accuracy criteria for these cross validation statistics are: (i) ME should be near or equal 0, (ii) RMSE should be near or equivalent to the standard deviation value of the sampled values and (iii) SMSE should be approximately close to one.

Spatial data analysis: The semivariogram of disease severity was computed using GS+ version 7 while kriging was performed using surfer version 8. Measured and kriged values were used to construct a spatial variability map of OS disease severity. Spatial dependence was represented as the ratio of nugget to sill and was interpreted as follows (Cambardella *et al*., 1994):

	Inference
Nugget:Sill<0.25	Strong spatial dependence
0.25<Nugget:Sill<0.75	Moderate spatial dependence
Nugget:Sill>0.75	Weak spatial dependence

RESULTS AND DISCUSSION

Descriptive statistics of OS disease severity is given in Table 1. The mean of OS disease severity is 24.24±0.8%. The Coefficient of Variation (CV) of OS disease severity is 83.34%. Transformation (log_{10} and l_n) of OS disease severity data did not alter the CV.

The distribution of OS disease severity is tailed to the right with a skewness coefficient of 0.62 and a kurtosis coefficient of -0.08 (Fig. 1). The Shapiro-Wilk normality test showed a W statistic of 0.93 that was significant at $p<0.05$, inferring that the OS disease severity data is not normally distributed.

Table 1: Descriptive statistics of OS disease severity

Parameters	Value
No.	587.00
Minimum	0.00
Maximum	92.30
Mean	24.24
Variance	407.05
Standard deviation	20.18
Median	23.69
Standard error	0.83
Coefficient of variance	83.34

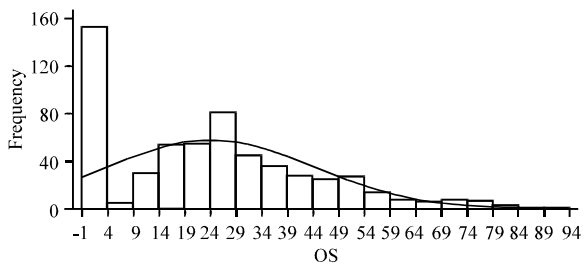

Fig. 1: Histogram of distribution of OS disease severity

Based on a total observation of 587 trees, OS incidence accounted for 74.3% of the study area while the remaining 25.7% did not exhibit OS symptoms. CCCVd-infected trees that do not exhibit OS symptoms are termed as asymptomatic. Randles (1998) reported that five out of ten asymptomatic trees observed in the Solomon Islands contained CCCVd-like molecules. There is a possibility that a portion or the entire 25.7% non-symptomatic trees in this study were in effect asymptomatic. Since OS symptoms were manifested on the majority of trees in the study area, spatial analysis of OS disease severity was made to include the data corresponding to non-symptomatic/asymptomatic trees. The spatial structure of OS disease severity is given in Fig. 2.

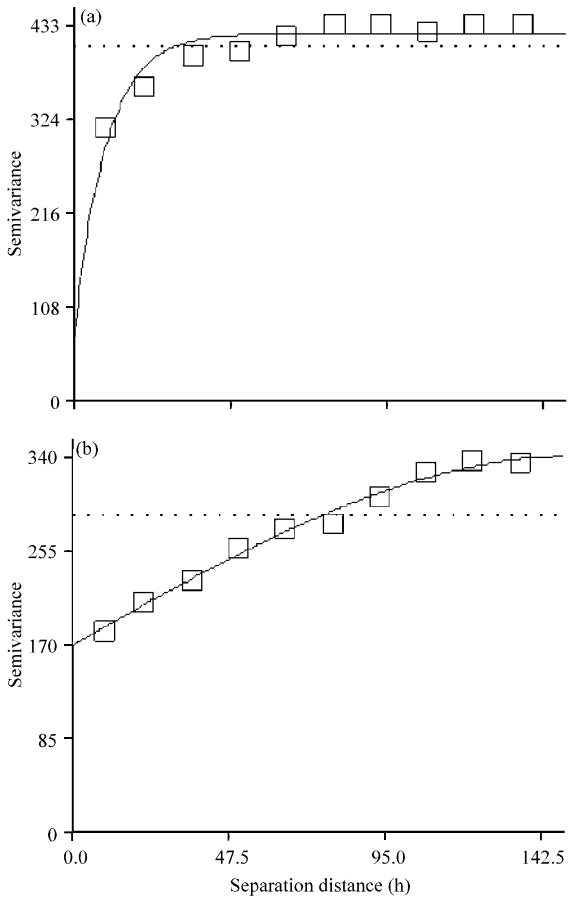

Fig. 2(a-b): Spatial structure of OS disease severity computed using, (a) Total dataset (n: 587, Model: Exponential, Spatial dependence: Strong, Nugget: 63.0, Sill: 421.3, Effective range: 29.1) and (b) Symptom-based dataset (n: 436, Model: Spherical, Spatial dependence: Moderate, Nugget: 170.2, Sill: 340.5, Effective range: 151.1)

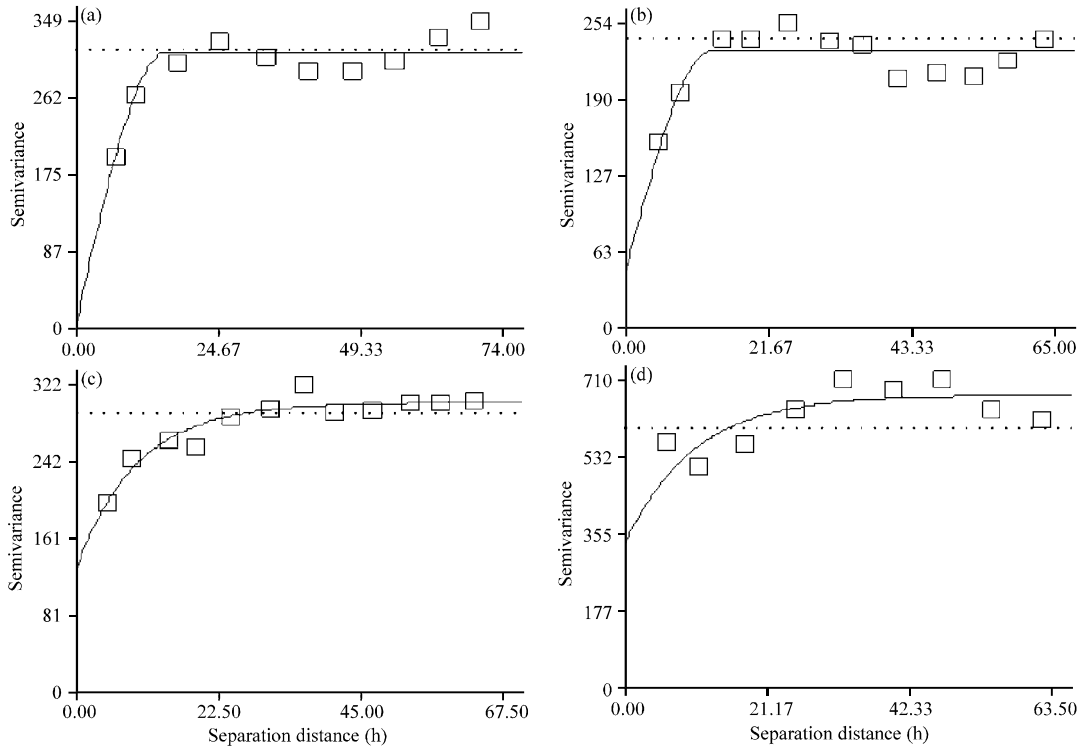

Fig. 3(a-d): Spatial structure and attributes of OS disease severity from (a) Sub-plot A (n: 155, Model: Spherical, Spatial dependence: Strong, Nugget: 2.5, Sill: 312.8, Effective range: 15.0 m), (b) Sub-plot B (n: 141, Model: Spherical, Spatial dependence: Strong, Nugget: 48.0, Sill: 229.8, Effective range: 13.0 m), (c) Sub-plot C (n: 155, Model: Exponential, Spatial dependence: Moderate, Nugget: 130.3, Sill: 302.7; Effective range: 28.8 m) and (d) Sub-plot D (n: 136, Model: Exponential, Spatial dependence: Moderate, Nugget: 336.0, Sill: 672.1, Effective range: 30.0 m)

Semivariograms shown in Fig. 2 were computed based on an active lag of 142.5 m and a lag class interval of 14.25 m. Active lag distance is 50% of the sampling area longest dimension and lag class interval is conventionally computed as 10% of the active lag distance value. The total dataset exhibits an exponential model with an effective range of 29.1 m, while the symptom-based dataset shows a spherical model with an effective range of 151.1 m. Sample points separated at distance greater than the effective range will no longer exhibit spatial autocorrelation (Balasundram *et al*., 2008). Sampling designs aimed at delineating spatial structures usually employ separation distances lesser than the effective range (Flatman and Yfantis, 1984). Spatial dependence of OS disease severity was stronger in the total dataset (Nugget:Sill of 0.15) as compared to symptom-based dataset (Nugget:Sill of 0.50). This physically means that the explainable proportion of total variation in OS disease severity for total dataset and symptom-based dataset is 85 and 50%, respectively. The higher nugget value for symptom-based dataset is possibly caused by the alteration of plot shape (i.e., less rectangular) resulting from the omission of 151 non-symptomatic/asymptomatic data points.

The total dataset and the symptom-based dataset fulfill all three cross-validation criteria (Table 2). Correlation between measured and kriged OS disease severity values of the total dataset and symptom-based dataset is 0.6 and 0.5, respectively. These validation assessments show that the accuracy of variography and interpolation for both datasets was acceptable. This suggests that, based on spatial distribution, the 25.7% of non-symptomatic trees that were possibly asymptomatic did not affect phytopathometry appraisal of OS disease. OS asymptomatic trees pose difficulty for disease severity evaluation via visual observation. In situations where the count of non-symptomatic trees which could be asymptomatic, are high, laboratory confirmation of OS disease incidence would be necessary.

Spatial distribution of OS disease severity could be varied within the study area. As such, the 4.2 ha study area was demarcated into four smaller plots, measuring approximately 1 ha each and subjected to semivariogram analysis. The spatial dependence of OS disease severity in the 1 ha sub-plots was strong for sub-plots A and B and moderate for sub-plots C and D (Fig. 3). Datasets from all four sub-plots fulfilled the cross-validation criteria (Table 3). The spatial structure of OS disease severity in

sub-plots A and B fitted a spherical model while that of sub-plots C and D fitted an exponential model. This result suggests that spatial structure and attributes of OS disease severity vary within the study site (Fig. 4).

The spatial variability map of OS disease severity is given in Figure 5. A large proportion of the study area (i.e., 73%) showed a low OS disease severity which ranged from 1 to 30%. High OS disease severity (>60%)

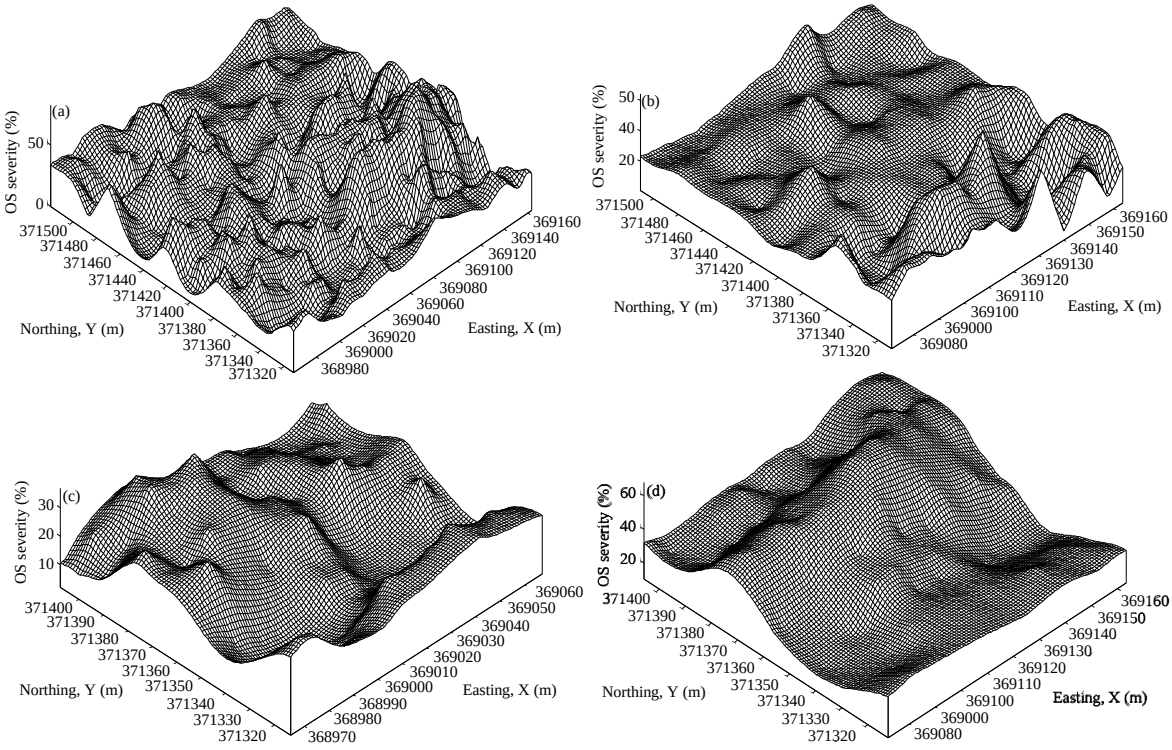

Fig. 4(a-d): Spatial variability of OS disease severity from the demarcated sub-plots (based on measured and kriged values), (a) Sub-plot A, (b) Sub-plot B, (c) Sub-plot C and (d) Sub-plot D; where Sub-plots A and B are adjacent to one another while Sub-plots C and D are adjacent to one another, and both the twin plots are divided by a plantation earth road

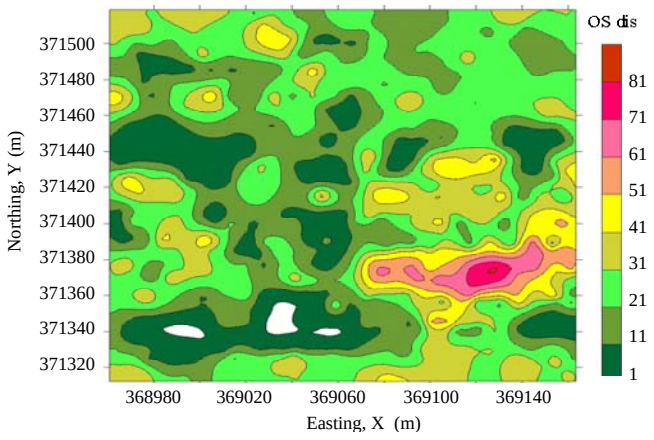

Fig. 5: Spatial variability of OS disease severity (based on measured and kriged values) with the corresponding areal distribution

Table 2: Cross validation statistics of interpolated values for OS disease severity

Data	No. of samples	Sample variance	ME	RMSE	SMSE
Total dataset	587	407.0467	-0.0905	324.5212	0.7986
Symptomatic dataset	436	288.0765	0.1135	197.6465	0.8234

Table 3: Cross validation statistics of interpolated values for OS disease severity from the demarcated sub-plots

Variables	Sample variance	ME	RMSE	SMSE
Sub plot A	315.8471	-0.3292	305.1929	0.9725
Sub plot B	240.4672	-0.4556	208.4480	0.8730
Sub plot C	293.1525	-0.0261	259.6795	0.8916
Sub plot D	599.5237	-0.0188	489.9920	0.8234

Table 4: Interpolated OS disease severity categories and corresponding aerial distribution

OS disease severity (%)	Area (m^2)	Area (%)
0	43.52	0.10
1-10	5861.48	14.00
11-20	10608.11	25.34
21-30	13865.68	33.12
31-40	7576.13	18.10
41-50	2219.17	5.30
51-60	919.08	2.20
61-70	562.90	1.35
71-80	187.26	0.45
>80	26.44	0.06
Total	41869.77	100.00

was observed south east of the study plot which accounted for almost 2% of the study area. The remaining 25% of the study area showed moderate OS disease severity that ranged from 31-60% (Table 4).

CONCLUSION

This study shows that the visually-observed incidence of Orange Spotting (OS) disease from a 15 year old oil palm stand is 74.3%. The spatial variability of OS disease severity was quantified at two levels of sample size which were: (i) total dataset with n = 587 and (ii) symptom-based dataset with n = 436. OS disease severity from the total dataset exhibited a strong spatial dependence that fitted an exponential model with an effective range of 29.1 m, while that of the symptom-based dataset showed a moderate spatial dependence that fitted a spherical model with an effective range of 151.1 m. Short-range variability of OS disease severity within smaller 1 ha sub-plots was also observed. Overall, results show that 73% of the study area has a low OS disease severity (1-30%). Another 25% of the study area has a moderate OS disease severity (31-60%, while the remaining 2% has a high severity (>60%).

Information about spatial clustering of OS disease severity could assist with OS phytopathometry appraisal. Such information is vital in designing site-specific disease monitoring and intervention strategies.

REFERENCES

Alves, C.M., F.M. Silva, E.A. Pozza and M.S. Oliveira, 2009. Modeling spatial variability and pattern of rust and brown eye spot in coffee agroecosystem. J. Pest Sci., 82: 137-148.

Balasundram, S.K., D.J. Mulla, P.C. Robert and D.L. Allan, 2006a. Accounting for spatial variability in a short-term fertilizer trial for oil palm. Int. J. Soil Sci., 1: 184-195.

Balasundram, S.K., P.C. Robert, D.J. Mulla and D.L. Allan, 2006b. Relationship between oil palm yield and soil fertility as affected by topography in an Indonesian plantation. Commun. Soil Sci. Plant Anal., 37: 1321-1337.

Balasundram, S.K., M.H.A. Husni and O.H. Ahmed, 2008. Application of geostatistical tools to quantify spatial variability of selected soil chemical properties from a cultivated tropical peat. J. Agron., 7: 82-87.

Cambardella, C.A., T.B. Moorman, J.M. Novak, T.B. Parkin, D.L. Karlen, R.F. Turco and A.E. Konopka, 1994. Field-scale variability of soil properties in central Iowa soils. Soil Sci. Soc. Am. J., 58: 1501-1511.

Cordier, T., C. Robin, X. Capdevielle, M.L. Desprez and C. Vacher, 2011. Spatial variability of phyllosphere fungal assemblages: Genetic distance predominates over geographic distance in a European beech stand (*Fagus sylvatica*). Fungal Ecol., (In Press). 10.1016/j.funeco.2011.12.004

Delhomme, J.P., 1978. Kriging in the hydrosciences. Adv. Water Resour., 1: 251-266.

Flatman, G.T. and A.A. Yfantis, 1984. Geostatistical strategy for soil sampling: The survey and the census. Environ. Monit. Assess., 4: 335-349.

Forde, S.C.M. and M.J.P. Leyritz, 1968. A study of confluent orange spotting of the oil palm in Nigeria. J. Nig. Inst. Oil Palm Res., 4: 371-380.

Gebbers, R. and V. Adamchuk, 2010. Precision agriculture and food security. Science, 327: 828-831.

Hanold, D. and J.W. Randles, 1991. Detection of coconut cadang-cadang viroid-like sequences in oil and coconut palm and other monocotyledons in south-west Pacific. Ann. Applied Biol., 118: 139-151.

Merino, G.G., D. Jones, D.E. Stooksbury and K.G. Hubbard, 2001. Determination of semivariogram models to krige hourly and daily solar irradiance in western Nebraska. J. Applied Meteorol., 40: 1085-1094.

Nutter, F.W., P.D. Esker and R.A.C. Netto, 2005. Disease assessment concepts and the advancements made in improving the accuracy and precision of plant disease data. Europ. J. Plant Pathol., 115: 95-103.

Paulitz, T.C., H. Zhang and R.J. Cook, 2003. Spatial distribution of *Rhizoctonia oryzae* and rhizoctonia root rot in direct-seeded cereals. Canad. J. Plant Pathol., 25: 295-303.

Price, W.C. and A.E. Bigornia, 1971. Incidence of cadang-cadang in three varieties of coconut trees of different ages. FAO Plant Protec. Bullet., 19: 136-137.

Price, W.C. and A.E. Bigornia, 1972. Evidence for spread of cadang-cadang disease of coconut from tree to tree. FAO Plant Protec. Bullet., 20: 133-135.

Randles, J.W. and M.J.B. Rodriguez, 2003. Coconut Cadang-Cadang Viroid. In: Viroids, Hadidi, A., R. Flores, J.W. Randles and J.S. Semancik (Eds.). Commonwealth Scientific and Industrial Research Organisation, Collingwood, Australia, ISBN-13: 978-0643067899, pp: 233-241.

Randles, J.W., 1998. CCCVd-Related Sequences in Species Other than Coconut. In: Report on ACIAR-Funded Research on Viroids and Viruses of Coconut Palm and Other Monocotyledons 1985-1993, Randles, J.W. and D. Hanold (Eds.). 51st Edn., Australian Centre for International Agricultural Research, Canberra, ISBN: 9781863202190, pp: 144-152.

Rekah, Y., D. Sberg and J. Katan, 1999. Spatial distribution and temporal development of fusarium crown and root of tomato and pathogen dissemination in field soil. Phytopathology, 89: 831-839.

Shibusawa, S., 1998. Precision farming and terra-mechanics. Proceedings of the 5th International Society for Terrain Vehicle Systems, Asia-Pacific Regional Conference, October 20-22, 1998, Seoul, Korea.

Sill, W.H. Jr., A.E. Bigornia and R.P. Pacumbaba, 1964. Incidence of cadang-cadang disease of coconut trees of different ages and its relationship to practical control. Philip. J. Plant Industry, 28: 87-102.

Vadamalai, G., A.A.F.L.K. Perera, D. Hanold, M.A. Rezaian and J.W. Randles, 2009. Detection of coconut cadang-cadang viroid sequences in oil and coconut palm by ribonuclease protection assay. Ann. Applied Biol., 154: 117-125.

Villate, L., V. Fievet, B. Hanse, F. Delemarre, O. Plantard, D. Esmenjaud and M. van Helden, 2008. Spatial distribution of the dagger nematode *Xiphinema* index and its associated *Grapevine fanleaf* virus in French vineyard. Phytopathology, 98: 942-948.